

Characterization of creep and crack growth interactions in the fracture behavior of concrete

Emmanuel Denarié^{a,*}, Christophe Cécot^b, Christian Huet^{c,✉}

^a *Laboratory of Maintenance, Construction and Safety of Structures, MCS-IS-ENAC,
EPFL—Ecole Polytechnique Fédérale de Lausanne, CH-1015, Lausanne, Switzerland*

^b *Expertises en mécanique et ingénierie, F-92360 Meudon-la-forêt, France; formerly at Laboratory of Building Materials,
LMC-IMX-STI, EPFL—Ecole Polytechnique Fédérale de Lausanne, CH-1015, Lausanne, Switzerland*

^c *Laboratory of Building Materials, LMC-IMX-STI, EPFL—Ecole Polytechnique Fédérale de Lausanne, CH-1015,
Lausanne, Switzerland*

Received 6 September 2005; accepted 13 November 2005

Abstract

Creep and crack growth govern the long-term deformability of concrete and thus its service behavior and its durability. The mechanisms involved in the couplings between these effects are not yet clearly identified. The aim of this research was to investigate experimentally and numerically at both the macro and the meso-level (heterogeneous material) the interactions between creep and crack growth in concrete and identify the main phenomena acting on the overall viscoelastic response of concrete, at various stages of fracture, during relaxations.

© 2005 Elsevier Ltd. All rights reserved.

Keywords: Microcracking; Creep; Finite element analysis; Micromechanics; Concrete

1. Introduction

Viscoelasticity and crack growth govern the long-term deformability of concrete and thus its service behavior and its durability. For low load levels, viscoelastic behavior appears quasi-linear and crack growth is inactive. On the other hand, for high load levels, cracks grow and interact with viscoelasticity. Numerous authors have long demonstrated qualitatively the influence of microcracking on creep. Moreover, rate effects on the fracture behavior of concrete are clear for low and high loading rates [1]. From recent research, it appears that only models taking into consideration both cohesive crack approaches extended to time dependent parameters and bulk viscoelasticity can reproduce the experimentally observed trends [2]. Nevertheless, the physical mechanisms involved in these effects are not yet clearly determined. The dissipative nature of crack growth and viscoelasticity naturally encourages

one to model their couplings by means of an energy-based approach to fracture. This is the meaning of the continuum thermodynamics of dissipative multicroaked granular bodies developed by Huet [3]. This theoretical formalism puts the emphasis on the effect of viscoelasticity on the driving (reactive) part of the propagation criteria (energy release rate).

The aim of this research was to investigate the couplings between viscoelasticity and crack growth in concrete, both experimentally and on the basis of numerical simulations at the meso and macro-level to search for clues for the observed effects. The experiments gave many indications of a significant role of microcrack propagation during relaxations at high load levels both near to and after the peak (maximum load). Moreover, the critical effect of the starting point of the relaxations (on the rupture envelope or under) was demonstrated. Relaxations started under the rupture envelope, even in the non-linear domain (around the peak), tend to produce significantly lower relative relaxations, with a distinctively different signature in a semi-log plot. The numerical simulations revealed some possible mechanisms to explain the observed trends. These mechanisms are clearly linked to the interactions between microcrack propagation, the viscoelastic

* Corresponding author. Tel.: +41 21 693 28 93; fax: +41 21 693 58 85.

E-mail address: emmanuel.denarie@epfl.ch (E. Denarié).

* Professor Huet passed away in October 2002. This paper was coauthored prior to his death and is published in his memory.

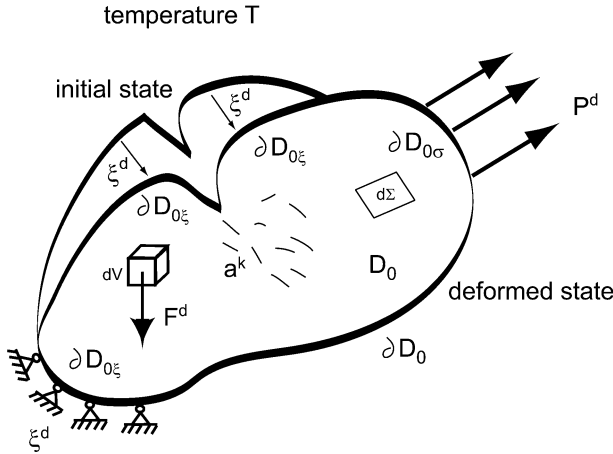


Fig. 1. Arbitrary system in initial and deformed state with applied solicitations.

behavior of the matrix, and the granular structure of concrete [3].

2. Theoretical background

Fig. 1 shows the two states (initial and deformed) of an arbitrary system, formed of a viscoelastic material and of a set of n microcracks (internal variables a_k for $k=1, n$), submitted to an arbitrary combination of solicitations in terms of displacements ξ^d imposed on the surface boundary $\partial D_{0\xi}$, surface forces P^d imposed on the surface boundary $\partial D_{0\sigma}$ and volumetric forces F^d imposed on volume D_0 . All imposed solicitations may vary with time.

The constitutive equations governing the evolution of the system are given in a very general way by the expression of the dissipation as a function of the variables of the problem. Huet [3] showed that for a multicroaked body, the propagation criteria for the k th crack tip geometry parameter can be expressed as:

$$G^k(a^k) = -\frac{\partial \Psi}{\partial a^k} = R_f^k \quad (1)$$

where G^k , energy release rate of the k th crack, and R_f^k : resistance to propagation or critical energy release rate of the k th crack. It should be noted that in this equation, the internal variables a^k are chosen in order to fully characterize the geometry and position of the microcracks. Depending on the configuration, they can be tensors (3D fracture planes).

Huet [4] introduced the so-called pseudo-convolutive operator \square defined as follows: if a and b are 2 tensors, the pseudo-convolution of a by b is given by:

$$c(t) = a \square b = \left(\int_{0_-}^t - \int_t^{2t^+} \right) a(2t-u) : db(u). \quad (2)$$

The total free energy of a linear viscoelastic body of volume V can be expressed, with the help of the Brun–Clapeyron formula, as [3]:

$$\Phi_\varepsilon(t) = \frac{1}{2} \int_{V_0} \left(\int_{0_-}^t - \int_t^{2t^+} \right) \sigma(2t-u) : d\varepsilon(u) dV \quad (3)$$

or, in its pseudo-convolutive form

$$\Phi_\varepsilon(t) = \frac{1}{2} \int_{D_0} \sigma \square \varepsilon dV \quad (4)$$

Using the pseudo-convolutive operator, Huet [3] showed that the potential energy can be written as:

$$\Psi_\varepsilon(t) = \frac{1}{2} \int_{\partial D_{0\xi}} P \square \xi^d d\Sigma - \frac{1}{2} \int_{\partial D_{0\sigma}} \xi \square P^d d\Sigma \quad (5)$$

The energy release rate for the k th crack tip is then given by:

$$G^{k,stat}(t) = -\frac{\partial \Psi_\varepsilon(t)}{\partial a_k} = \frac{1}{2} \int_{\partial D_{0\sigma}} \frac{\partial \xi}{\partial a_k} \square P^d d\Sigma - \frac{1}{2} \int_{\partial D_{0\xi}} \frac{\partial P}{\partial a_k} \square \xi^d d\Sigma \quad (6)$$

This expression applies for any non-aging linear viscoelastic body provided that body forces and kinetic energy terms can be neglected (onset of propagation or slow crack growth) and that the lips of the considered crack are force-free. In order to simulate the couplings between viscoelasticity and microcrack propagation for a granular microcracked body with a viscoelastic matrix, it has been implemented in a finite element code by Cécot [5].

3. Experimental

The tests have been performed with a Wedge Splitting System (WST) inspired from the one developed by Brühwiler [6], Fig. 2. One single type of material (concrete, river

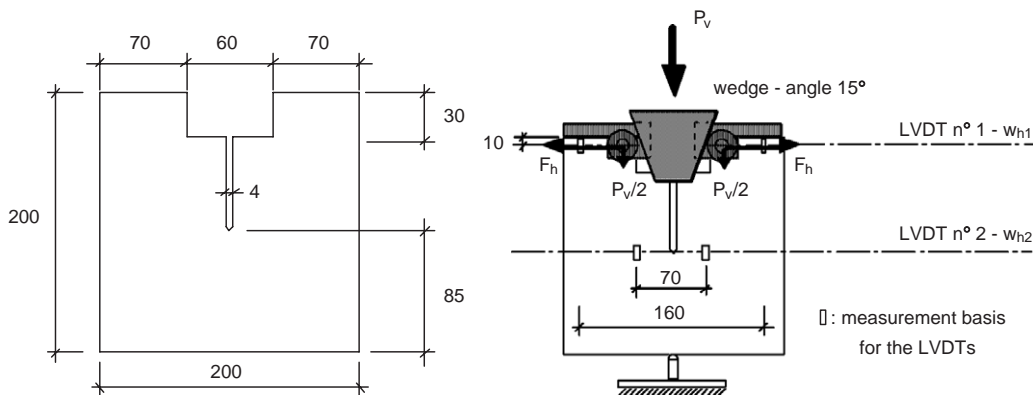


Fig. 2. Wedge Splitting Test (WST), specimen (thickness: 97 mm) and testing set-up.

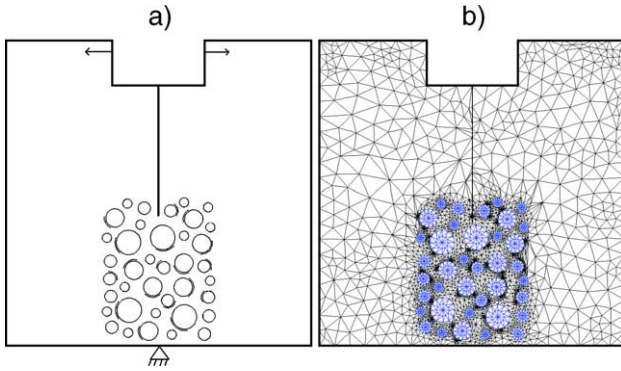


Fig. 3. a) Granular microcracked structure, and b) FEM mesh of a WST specimen.

aggregates 0/8 mm, 460 kg/m³ of OPC type CEM I 42.5, W/C=0.43, $f_{cw,28}$ = 50 N/mm², age at testing between 50 and 100 days) has been used. All specimens were protected from desiccation by a paraffin based curing compound. Two series of LVDTs were used. One in the axis of the horizontal splitting force F_h (reference w_{h1}) and one at the level of the prenotch tip (reference w_{h2}). On some specimens, acoustic emission sensors and a conductive graphite surface crack gauge have also been used [7]. Tests were run in closed-loop displacement control (either w_{h1} or w_{h2}) in a servo hydraulic testing system. The relaxations were imposed successively, at various load levels, starting before the peak. Different values of the load level at first relaxation have been used (M11914: 38%, M12022: 85%, M12213: 40%).

4. Numerical model

The computer code originally developed by Wang [8] for the simulation of crack propagation in a microcracked granular elastic media, and modified by Cécot [5] to take into consideration the bulk viscoelasticity (linear) of the matrix, has been used. Crack propagation was simulated by means of an energy based criteria [9], corresponding to the formulation introduced in Section 2. Fig. 3 shows a) the heterogeneous structure and b) a typical mesh generated by the program.

5. Results and discussion

In the following, for obvious reasons, the observed effects will be illustrated only for a reduced number of specimens. All these effects could be replicated on several other specimens, detailed results can be found in [7]. Fig. 4 shows the relative relaxations obtained for specimen M11914 with a control of w_{h1} , both pre- and post-peak. On the figures, the number of the relaxation is followed by the load level (% of the peak load). Pre-peak, Fig. 4a, all relaxations after no. 1, till no. 5, were performed with a constant displacement increment from one level to the other. For a purely linear viscoelastic material, in such a case, theory predicts relative relaxations less and less pronounced. This trend is respected till relaxation no. 2 (at 48%). Starting with relaxation no. 3 (at 60%), all successive ones follow an opposite trend (relaxations more and more pronounced), which reveals a progressive deviation from linearity when one approaches the absolute peak of force. Post-peak, Fig. 4b, the relative relaxations tend to merge whatever the load level and to follow a typical behavior (linear in a semi-log plot) already observed by Bažant and Gettu [10] on 3 PTB specimens.

Fig. 5 (specimen M12022) shows the response for relaxations with a control of w_{h1} , with a first level at 85% of the maximal load. On the experimental load–displacement curve, Fig. 5a, one can notice that among all the relaxations, no. 5 is the only one to start clearly under the rupture envelope. In Fig. 5b, the relative relaxations after the peak show the same trend as for specimen M11914, except for no. 5 for which the relaxation is much less pronounced than the ones for nos. 4 and 6. Moreover, the signature of this relaxation curve in a semi-log plot is very distinct (marked curvature) from the linear shape obtained for nos. 4 and 6 (as observed in the post-peak range for specimen M11914). One can relate this special behavior to the fact that relaxation no. 5 is performed under the rupture envelope. For comparison, the relative relaxations predicted by a linear viscoelastic simulation (homogeneous material, no crack propagation) using the FEM code developed by Cécot [5] have been plotted in the same figure. It can be seen that experimental relaxation no. 5 is much closer to the simulated linear viscoelastic behavior than experimental relaxation nos. 4 and 6, although no. 5 shows a clear non-linear deviation. From

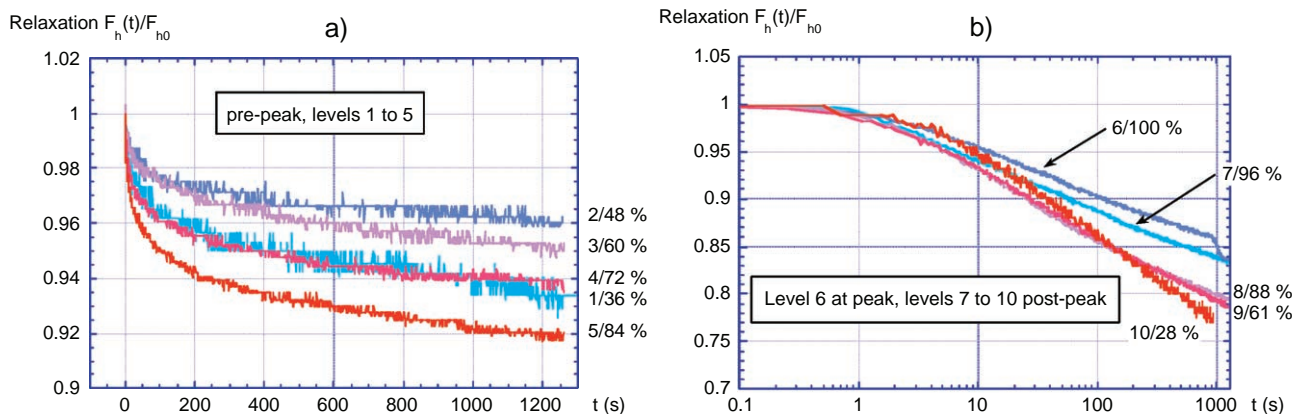


Fig. 4. Specimen M11914, control w_{h1} , relative relaxations, a) pre-peak, b) post-peak.

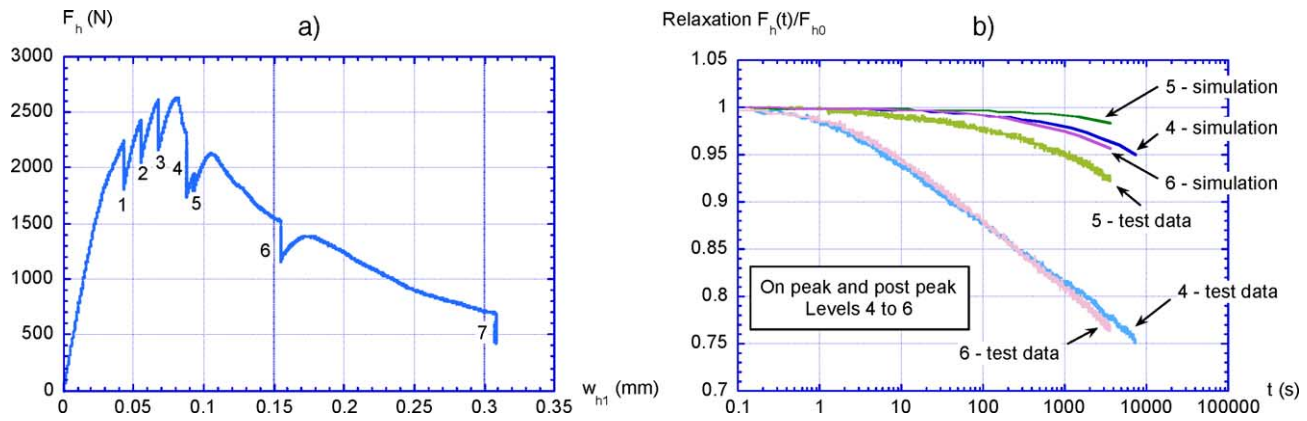


Fig. 5. Specimen M12022, control w_{h1} , a) Force–displacement w_{h1} , b) relative relaxations, steps 4, 5, 6 near and after the peak, experimental results and simulations (linear viscoelasticity).

this, it appears that in the post peak range (with ongoing damage), performing relaxations on the rupture envelope or clearly under it could activate different mechanisms thus explaining the great differences observed.

These mechanisms could be related to progression of damage during relaxations performed on the rupture envelope, namely microcrack propagation during the relaxations.

In order to get confirmation that the occurrence of microcrack propagation during relaxations started on the rupture envelope, acoustic emission measurements have been performed on a specimen (M12213) submitted to a loading program similar to the one of specimen M11914. Fig. 6 shows the load vs. time curves of specimen M12213 together with the occurrence of acoustic events (circles) plotted with the same load vs. time scale. On the same figure, the evolution of the projected crack length measured on the surface of the specimen by a conductive graphite gauge has also been plotted. In Fig. 6a, one can see the complete curves. The crack gauge reacts to the increase of displacement between the relaxations but shows no significant variation of crack length during the relaxations. On the contrary, AE can be detected both between the relaxations and during some of them, mostly at the beginning. During relaxation no. 1 (load level=40% of peak), various AE events can be detected. Then, before the peak, till relaxation no. 4, no more. From the peak on, all relaxations are

accompanied by AE events that tend to vanish during the load decrease. Fig. 6b shows clearly the AE events occurring at the beginning of relaxation nos. 4 and 5, close to the peak. These observations give support to the presence of an active microcracking at least at the beginning of relaxations performed on the rupture envelope, in the peak and post-peak ranges.

Microcrack propagation is expected and has been observed during creep tests by many authors. In a relaxation test, it was not expected. Theoretically, for a homogeneous material, relaxation implies a decrease of the energy release rate G , which is the driving force for crack propagation [3]. Unless the resistance to crack propagation decreases faster than G , crack propagation is impossible. One possible justification of the experimentally observed phenomena could be found in the heterogeneous microstructure (granulates and preexisting microcracks) of concrete. Fig. 7 illustrates the results of a numerical simulation of the processes involved in a WST specimen, in the FPZ, at the beginning of a relaxation (zoom on notch tip). Let us assume that prior to the blocking of the displacement w_{h1} (beginning of the relaxation), microcracks continuously propagate in an unstable way due to their small size. Let us further assume that just when the relaxation starts, one single microcrack (1) (as illustrated in Fig. 7a) was propagating and that its propagation ends after the relaxation

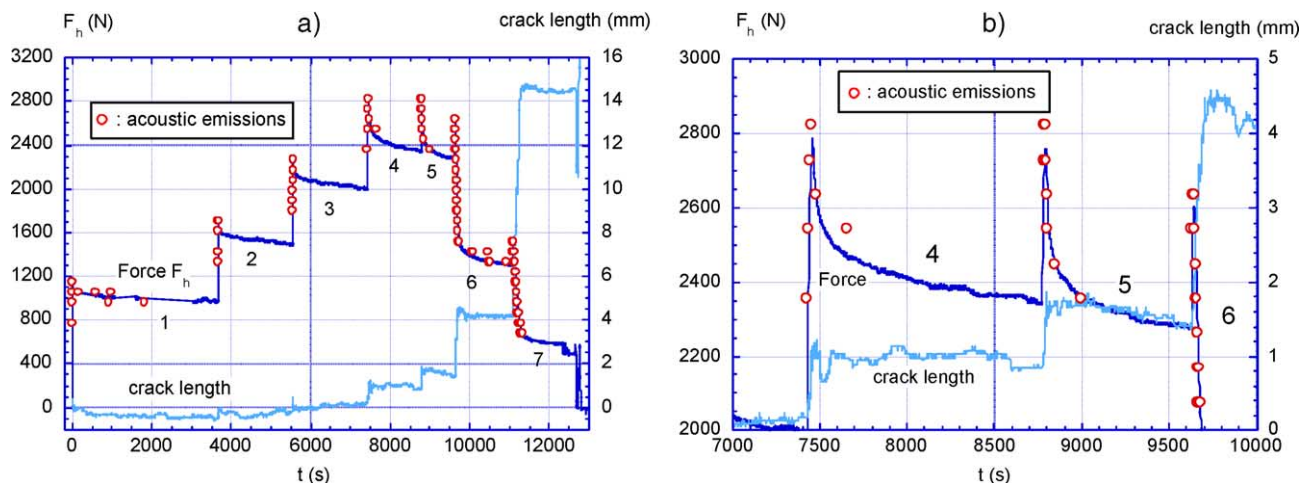


Fig. 6. Specimen M12213, control w_{h1} , absolute relaxations with Acoustic Emission (AE) events and crack length vs. time, a) general, b) detail on the peak.

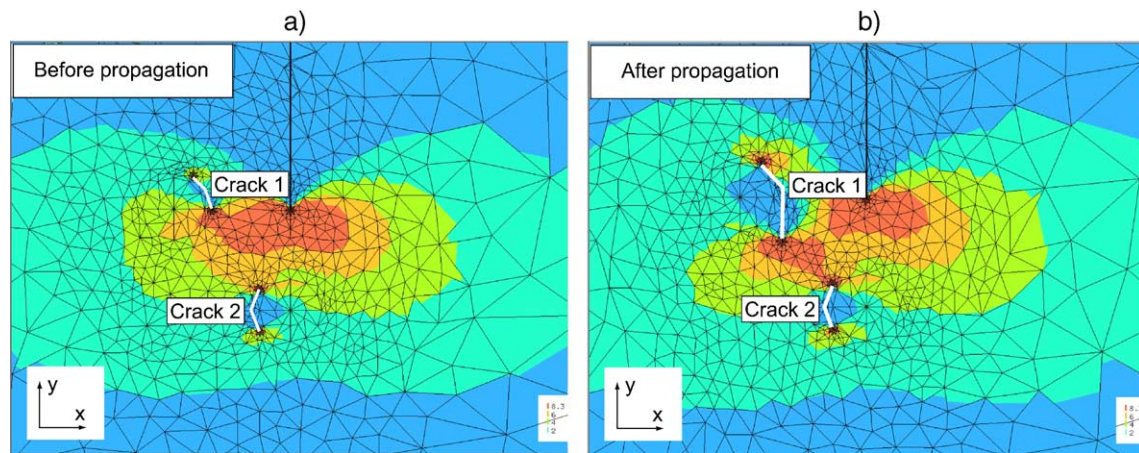


Fig. 7. Simulation of the interaction of microcracks in the Fracture Process Zone (FPZ), near the notch tip of a WST specimen, during relaxation; stress field σ_{xx} .

started. Owing to the heterogeneous microstructure of concrete the propagating microcrack will modify the stress field of neighboring microcracks in the FPZ and as shown in Fig. 7b even induce the propagation of microcrack (2), even if the load decreased. This process can be replicated till the load relaxation excludes all new propagation. In this way, the vicinity of microcracks in the FPZ could explain the chain reactions of propagations even during a relaxation. The key point is the intrinsic unstable nature of the microcracks due to their small size and their vicinity in the FPZ.

6. Conclusions

The viscoelastic response of concrete Wedge Splitting Specimens submitted to successive relaxations, both in the pre- and post-peak range, in a fracture test, has been investigated.

- With this test method, pre-peak, one can characterize accurately the progressive shift from a linear viscoelastic behavior, starting at around 50% of the peak load for this specimen type and size.
- Post-peak, the relaxations initiated at the rupture envelope tend, in a relative load scale, to merge for all load levels and show a distinct signature (linear in a semi-log plot), agreeing with the previous observations of Bažant and Gettu [10].
- Post-peak, the relaxations initiated under the rupture envelope show a very distinct behavior with less pronounced relative values. This could provide a means for isolating possible contributions of microcrack propagation in the non-linear viscoelastic behavior of concrete.
- Many indices of microcrack propagation during relaxations in the near-peak and post-peak range were directly observed (Acoustic Emissions).

Numerical simulations taking into consideration the heterogeneous microstructure of concrete at the meso-level and the viscoelastic behavior of the matrix can explain the effects observed. They reveal possible phenomena of interaction of microcracks in the FPZ that could lead to chain reactions of successive unstable propagations during relaxations, even if the externally measured load decreases at the same time.

Significant contributions of microcracks propagations on the load decrease during relaxations should be taken into consideration when evaluating the non-linear viscoelastic properties of concrete. Otherwise, the beneficial effects of viscoelasticity on the long term behavior of concrete structures could be overestimated.

Acknowledgement

The authors wish to thank Lucie Baillon (LMC-IMX-EPFL) for having performed the acoustic emission measurements.

References

- [1] Z.P. Bažant, W.H. Gu, K.T. Faber, Softening reversal and other effects of a change in loading rate on fracture of concrete, *ACI Mater. J.* (Jan.–Feb. 1995) 3–9.
- [2] Y.N. Li, Z.P. Bažant, Cohesive crack model with rate-dependent opening and viscoelasticity: II. Numerical algorithm, behavior and size effect, *Int. J. Fract.* 86 (1997) 267–288.
- [3] C. Huet, An integrated micromechanics and statistical continuum thermodynamics approach for studying the fracture behavior of microcracked heterogeneous materials with delayed response, *Eng. Fract. Mech.* 58 (5,6) (1997) 459–556.
- [4] C. Huet, Minimum theorems for viscoelasticity, *Eur. J. Mech. A, Solids* 11 (5) (1992) 653–684.
- [5] C. Cécot, Etude micromécanique par simulation numérique en éléments finis des couplages viscoélasticité-croissance des fissures dans les composites granulaires de type béton, Doctoral Thesis no. 2365, Swiss Federal Institute of Technology, Lausanne (2001).
- [6] E. Brühwiler, Bruchmechanik von Staumauerbeton unter Quasi-Statistischer und Erdbebendynamischer Belastung, Doctoral Thesis no. 739, Swiss Federal Institute of Technology, Lausanne (1988).
- [7] E. Denarié, Etude expérimentale des couplages viscoélasticité-croissance des fissures dans les bétons de ciment, Doctoral Thesis no. 2195, Swiss Federal Institute of Technology, Lausanne (2000).
- [8] J. Wang, Development and Application of a Micromechanics-based Numerical Approach for the Study of Crack propagation in Concrete, Doctoral Thesis no. 1233, Swiss Federal Institute of Technology, Lausanne (1994).
- [9] C. Cécot, C. Huet, Numerical simulations of viscoelastic effects in concrete crack growth, in: F. Miannay, P. Costa, D. François, A. Pineau (Eds.), *Advances in mechanical behavior, plasticity and damage, Proc. EURO-MAT 2000*, vol. 1, Elsevier, 2000, p. 747.
- [10] Z.P. Bažant, R. Gettu, Rate effects and load relaxation in static fracture of concrete, *ACI Mater. J.* 89 (5) (Sept.–Oct. 1992) 456.